Commun. Theor. Phys. **75** (2023) 125502 (9pp) https://doi.org/10.1088/1572-9494/ad0f8d

Disassociation of a one-dimensional cold molecule via quantum scattering

Wen-Liang Li[1,2], **Hai-Jing Song**[3], **Tie-Ling Song**[4] and **D L Zhou**[1,2]

[1] Institute of Physics, Beijing National Laboratory for Condensed Matter Physics, Chinese Academy of Sciences, Beijing 100190, China
[2] School of Physical Sciences, University of Chinese Academy of Sciences, Beijing 100049, China
[3] National Innovation Institute of Defense Technology, AMS, Beijing 100071, China
[4] Department of Fundamental Science, Space Engineering University, Beijing 101416, China

E-mail: zhoudl72@iphy.ac.cn

Received 18 July 2023, revised 5 November 2023
Accepted for publication 24 November 2023
Published 20 December 2023

Abstract

Motivated by the recent experimental developments in ultracold molecules and atoms, we propose a simple theoretical model to address the disassociation, reflection, and transmission probability of a one-dimensional cold molecule via quantum scattering. First, we show the Born approximation results in the weak interaction regime. Then, by employing the Lippmann–Schwinger equation, we give the numerical solution and investigate the disassociation's dependence on the injection momentum and the interaction strengths. We find that the maximum disassociation rate has a limit when increasing the interaction strengths and injection momentum. We expect that our model can be realized in experiments in the near future.

Keywords: cold molecule, quantum scattering, disassociation rate

(Some figures may appear in colour only in the online journal)

1. Introduction

Laser cooling makes atoms or molecules ultracold, e.g. the temperature may arrive at the regime of nano-Kelvin [1–5], which results in the emergence of quantum features of the atoms or molecules, which are usually hidden in the thermal noises from the environments. Thus, the ultracold atoms or molecules become an ideal platform for investigation of fundamental quantum mechanics problems, quantum chemistry, precise quantum metrology, quantum simulations, and even quantum computing [6–13].

Among these applications, ultracold chemistry is closely related to laser-cooled atoms or molecules [14, 15]. Along this direction, one-dimensional ultracold atoms/molecules, which are formed by a tight confinement with a wave guide [16], play a crucial role due to their relatively simple theoretical model with rich physics [17].

Currently, different kinds of molecules formed from several atoms have been investigated intensively in the literature [18–21]. However, the converse process, i.e. the disassociation of molecules into atoms, deserves further studies to deepen its understanding. Here, we propose a simple theoretical model to address the disassociative probability of a one-dimensional cold molecule, and investigate its dependence on the injection momentum and the interaction strengths, which can be arbitrarily tuned via the Feshbach resonance technique [22, 23]. Our results show that there is a limit of the maximum disassociation rate when increasing both the injection momentum and interaction strengths.

This article is structured as follows: in section 2, we introduce our theoretical model of the scattering problem and give the Hamiltonian. In section 3, we give the eigenstates and the in state of our scattering. Then, we solve the model and show our numerical results by applying Born approximation in section 4 and an integral equation method in section 5. Finally, we present our discussion and conclusions in section 6.

2. The model

We consider a one-dimensional molecule, which is the unique weakly bound state formed by an attractive one-dimensional contact interaction. Then, the one-dimensional molecule

scatters with a heavy atom. The Hamiltonian of our system is modeled by

$$H = \frac{p_1^2}{2m_1} + \frac{p_2^2}{2m_2} - \alpha\delta(x_2 - x_1) + \gamma_1\delta(x_1) + \gamma_2\delta(x_2), \tag{1}$$

where m_1, m_2 are the masses of the two particles, p_1, p_2 are their momentum operators, and x_1, x_2 are their position operators in one dimension. Here, α, γ_1, $\gamma_2 > 0$ are interaction strengths of the three contact potentials, where $\alpha\delta(x_2 - x_1)$ represents the contact potential between particle 1 and particle 2, $\gamma_1\delta(x_1)$ represents the contact potential between particle 1 and particle 3, and $\gamma_2\delta(x_2)$ represents the contact potential between particle 2 and particle 3. Here, we assume that the position of particle 3—a heavy atom—is at zero, and the motion of the heavy atom is neglected.

To solve the scattering problem, we split the Hamiltonian into two parts:

$$H = H_0 + V, \tag{2}$$

where

$$H_0 = \frac{P^2}{2M} + \frac{p^2}{2\mu} - \alpha\delta(x), \tag{3}$$

$$V = \gamma_1\delta(X - r_2x) + \gamma_2\delta(X + r_1x), \tag{4}$$

with

$$r_1 = \frac{m_1}{M}, \tag{5}$$

$$r_2 = \frac{m_2}{M}, \tag{6}$$

$$M = m_1 + m_2 = (r_1 + r_2)M, \tag{7}$$

$$\mu = \frac{m_1m_2}{M} = r_1r_2M, \tag{8}$$

$$\kappa = \sqrt{r_1r_2} = \sqrt{\frac{\mu}{M}}, \tag{9}$$

$$X = \frac{m_1x_1 + m_2x_2}{M} = r_1x_1 + r_2x_2, \tag{10}$$

$$x = x_2 - x_1, \tag{11}$$

$$P = M\dot{X} = p_1 + p_2, \tag{12}$$

$$p = \mu\dot{x} = r_1p_2 - r_2p_1. \tag{13}$$

Through this coordinate transformation, we rewrite the Hamiltonian as the representation of the center-of-mass coordinate X and relative coordinate x, where M is the total mass of the two particles and μ is the reduced mass. Then, P is the total momentum and p is the relative momentum.

3. The in state of our scattering

In this section, we will examine the in state of our scattering. Let us start with the eigen problem of H_0, which can be divided into two parts:

$$H_0 = H_0^c + H_0^r, \tag{14}$$

where

$$H_0^c = \frac{P^2}{2M}, \tag{15}$$

$$H_0^r = \frac{p^2}{2\mu} - \frac{q}{\mu}\delta(x) \tag{16}$$

with $q = \mu\alpha$. Note that H_0^c is the kinetic energy of the center of mass for the two atoms, and H_0^r is the energy of their relative motion. Thus, $[H_0^c, H_0^r] = 0$, and the eigen problem of H_0 can be solved by finding the common eigenstates of ${H_0}^c$ and H_0^r.

The eigen equation of H_0^c is given by

$$H_0^c|P\rangle = \frac{P^2}{2M}|P\rangle, \tag{17}$$

where the eigen wave function is

$$\langle X|P\rangle = \frac{1}{\sqrt{2\pi}}\mathrm{e}^{\mathrm{i}PX}. \tag{18}$$

The eigen equation of H_0^r is

$$H_0^r|\phi_b\rangle = E_b|\phi_b\rangle, \tag{19}$$

$$H_0^r|\phi_{p+}\rangle = E_p|\phi_{p+}\rangle, \tag{20}$$

where $|\phi_b\rangle$ is the unique bound state with energy $E_b = -\frac{q^2}{2\mu}$, and the wave function for the bound state

$$\langle x|\phi_b\rangle = \sqrt{q}\,\mathrm{e}^{-q|x|}. \tag{21}$$

The eigenstate $|\phi_{p+}\rangle$ is the scattering state with respect to H_0^r with energy $E_p = \frac{p^2}{2\mu}$, and the wave function is

$$\langle x|\phi_{p+}\rangle = \begin{cases} \frac{1}{\sqrt{2\pi}}\left[\left(\mathrm{e}^{\mathrm{i}px} + \frac{\mathrm{i}q}{p - \mathrm{i}q}\mathrm{e}^{-\mathrm{i}px}\right)\theta(-x) + \left(\frac{p}{p - \mathrm{i}q}\mathrm{e}^{\mathrm{i}px}\right)\theta(x)\right], & p > 0, \\ \frac{1}{\sqrt{2\pi}}\left[\left(\mathrm{e}^{\mathrm{i}px} + \frac{\mathrm{i}q}{-p - \mathrm{i}q}\mathrm{e}^{-\mathrm{i}px}\right)\theta(x) + \left(\frac{-p}{-p - \mathrm{i}q}\mathrm{e}^{\mathrm{i}px}\right)\theta(-x)\right], & p < 0. \end{cases} \tag{22}$$

Here, we observe that $\langle x|\phi_{(-p)+}\rangle = \langle -x|\phi_{p+}\rangle$, i.e. $\langle -x|\phi_{p+}\rangle$ is also an eigenstate of H_0^r, which results from the symmetry of space inversion of H_0^r, i.e. the Hamiltonian is invariant under $x \to -x$. In the Hilbert space of the relative motion, we can show the following complete relation

$$\int_{-\infty}^{+\infty} \mathrm{d}p|\phi_{p+}\rangle\langle\phi_{p+}| + |\phi_b\rangle\langle\phi_b| = 1. \tag{23}$$

Now we are ready to give the in state of our scattering

$$|\Psi_{\text{in}}\rangle = |P\rangle \otimes |\phi_b\rangle \equiv |P, \phi_b\rangle, \tag{24}$$

which describes a one-dimensional molecule in the bound state $|\phi_b\rangle$ scattering on the potential V with the momentum of the mass center P.

4. Born approximation in the molecule channel

In this section, we will apply the Born approximation to our scattering problem. We start with the Lippmann–Schwinger equation:

$$|\Phi^+_{P,b}\rangle = |P, \phi_b\rangle + G^+(E_P)V|P, \phi_b\rangle \tag{25}$$

$$=|P, \phi_b\rangle + G_0^+(E_P)V|\Phi^+_{P,b}\rangle, \tag{26}$$

where the Green function and the free Green function are given by

$$G^+(E) = \frac{1}{E - H + \mathrm{i}\epsilon}, \tag{27}$$

$$G_0^+(E) = \frac{1}{E - H_0 + \mathrm{i}\epsilon}. \tag{28}$$

Therefore, the S matrix in the molecule channel is

$$\langle Q, b|S|P, b\rangle = \langle \Phi^-_{Q,b}|\Phi^+_{P,b}\rangle \tag{29}$$

$$= \delta(P - Q) - 2\pi\mathrm{i}\delta(E_Q - E_P)\langle Q, \phi_b|V|\Phi^+_{P,b}\rangle. \tag{30}$$

The out scattering state in the molecule channel is

$$\begin{aligned}|\Psi_{\text{out}}\rangle_b &= \int_{-\infty}^{\infty} \mathrm{d}Q|Q, \phi_b\rangle\langle Q, \phi_b|S|P, \phi_b\rangle \\ &= \left(1 - \mathrm{i}\frac{2\pi M}{P}\langle P, \phi_b|V|\Phi^+_{P,b}\rangle\right)|P, \phi_b\rangle \\ &\quad - \mathrm{i}\frac{2\pi M}{P}\langle -P, \phi_b|V|\Phi^+_{P,b}\rangle|-P, \phi_b\rangle.\end{aligned} \tag{31}$$

Then, the reflection rate and the transmission rate for the molecule are

$$R_b = \frac{4\pi^2M^2}{P^2}\,|\langle -P, \phi_b|V|\phi^+_{P,b}\rangle|^2, \tag{32}$$

$$\begin{aligned}T_b = 1 &+ \frac{4\pi^2M^2}{P^2}\,|\langle P, \phi_b|V|\phi^+_{P,b}\rangle|^2 \\ &+ \frac{4\pi M}{P}\,\mathrm{Im}\{\langle P, \phi_b|V|\phi^+_{P,b}\rangle\}.\end{aligned} \tag{33}$$

Therefore, in the Born approximation up to the second order of V:

$$R_b = \frac{4\pi^2M^2}{P^2}\,|\langle -P, \phi_b|V|P, \phi_b\rangle|^2, \tag{34}$$

$$\begin{aligned}T_b = 1 &+ \frac{4\pi^2M^2}{P^2}\,|\langle P, \phi_b|V|P, \phi_b\rangle|^2 \\ &+ \frac{4\pi M}{P}\,\mathrm{Im}\{\langle P, \phi_b|VG_0^+(E_P)V|P, \phi_b\rangle\}.\end{aligned} \tag{35}$$

Note that

$$\begin{aligned}G_0^+(E_p) &= \frac{1}{E_P + E_b - H_0 + \mathrm{i}\epsilon} \\ &= \mathcal{P}\frac{1}{E_P + E_b - H_0} - \mathrm{i}\pi\delta(E_P + E_b - H_0).\end{aligned} \tag{36}$$

Thus

$$\begin{aligned}&\mathrm{Im}\{\langle P, \phi_b|VG_0^+(E_P)V|P, \phi_b\rangle\} \\ &= -\pi\langle P, \phi_b|V\delta(E_P + E_b - H_0)V|P, \phi_b\rangle \\ &= -\pi\int \mathrm{d}Q\delta(E_P - E_Q)|\langle Q, \phi_b|V|P, \phi_b\rangle|^2 \\ &\quad -\pi\int \mathrm{d}Q\int \mathrm{d}p\delta(E_P + E_b - E_Q - E_p) \\ &\quad |\langle Q, \phi_{p+}|V|P, \phi_b\rangle|^2 \\ &= -\frac{\pi M}{P}(|\langle P, \phi_b|V|P, \phi_b\rangle|^2 \\ &\quad + |\langle -P, \phi_b|V|P, \phi_b\rangle|^2) \\ &\quad -\int_{-p_{\max}}^{p_{\max}} \mathrm{d}p\frac{\pi M}{Q(p)}(|\langle Q(p), \phi_{p+}|V|P, \phi_b\rangle|^2 \\ &\quad + |\langle -Q(p), \phi_{p+}|V|P, \phi_b\rangle|^2),\end{aligned} \tag{37}$$

where $Q(p) = \sqrt{p^2_{\max} - p^2}\,\big/\kappa$ with $p_{\max} = \sqrt{\kappa^2P^2 - q^2}$.

Hence, we find

$$T_b = 1 - R_b - C_{nb}, \tag{38}$$

where

$$\begin{aligned}C_{nb} = &\frac{4\pi^2M^2}{P}\int_{-p_{\max}}^{p_{\max}} \mathrm{d}p \\ &\times \frac{|\langle Q(p), \phi_{p+}|V|P, \phi_b\rangle|^2 + |\langle -Q(p), \phi_{p+}|V|P, \phi_b\rangle|^2}{Q(p)}.\end{aligned} \tag{39}$$

Equation (38) implies that C_{nb} is the disassociation rate, i.e. the rate that the molecule becomes two atoms after the scattering. In addition, only when $P > \frac{q}{\kappa}$ is C_{nb} positive.

From detailed calculations, we obtain

$$R_b = \frac{M^2q^4}{P^2}\left(\frac{\gamma_1}{q^2 + r_2^2P^2} + \frac{\gamma_2}{q^2 + r_1^2P^2}\right)^2, \tag{40}$$

and

$$\begin{aligned}&|\langle Q, \phi_{p+}|V|P, \phi_b\rangle|^2 = \left(\frac{q}{2\pi}\right)^3\frac{16(P - Q)^2p^2}{p^2 + q^2} \\ &\times\left(\frac{1}{[p + (P - Q)r_2]^2 + q^2}\left(\frac{r_2\gamma_1}{[(P - Q)r_2 - p]^2 + q^2}\right)^2\right. \\ &+ \frac{1}{[p + (P - Q)r_1]^2 + q^2}\left(\frac{r_1\gamma_2}{[(P - Q)r_1 - p]^2 + q^2}\right)^2 \\ &+ \frac{r_2\gamma_1}{[(P - Q)r_2 - p]^2 + q^2}\frac{r_1\gamma_2}{[(P - Q)r_1 - p]^2 + q^2} \\ &\times\left.\frac{2[p + (P - Q)r_2][p + (P - Q)r_1] + 2q^2}{([p + (P - Q)r_2]^2 + q^2)([p + (P - Q)r_1]^2 + q^2)}\right),\end{aligned} \tag{41}$$

which can be inserted into equation (39) to numerically calculate the disassociation rate C_{nb}.

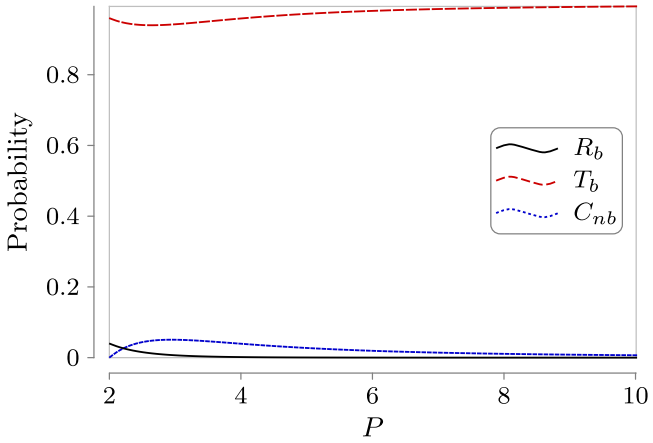

Figure 1. Disassociation under the Born approximation. Here, the parameters are given by $m_1 = m_2 = 1.0$, $\gamma_1 = \gamma_2 = 0.2$, and $\alpha = 2.0$.

Now we are ready to present our numerical results on the transmission rate T_b, the reflection rate R_b, and the disassociation rate C_{nb} in the first-order Born approximation in figure 1. Here, the parameters are given by $m_1 = m_2 = 1.0$, $\gamma_1 = \gamma_2 = 0.2$, and $\alpha = 2.0$. Due to the energy conservation, only when the mass-center momentum $P > 2$ does the disassociation process occur. With the increase in the momentum P, the transmission rate T_b increases while the reflection rate R_b decreases. In particular, the disassociation rate C_{nb} take its maximum $\simeq 0.05$ at $P \simeq 2.9$.

5. Integral equation method

Note that Born approximation is valid only when the momentum P is large, and the interaction strengths γ_1 and γ_2 are small. To obtain more general information on the disassociation process, we may resort to the direct numerical solution of the Lippmann–Schwinger equation.

From equations (34), (35), we need to calculate $V|\Phi^+_{P,b}\rangle$, which can be obtained from the Lippmann–Schwinger equation (25) and satisfies

$$(1 - VG_0^+(E_P))V|\Phi^+_{P,b}\rangle = V|P, \phi_b\rangle. \tag{42}$$

Therefore we arrives at the integral equation

$$\begin{pmatrix} |\Phi^1\rangle \\ |\Phi^2\rangle \end{pmatrix} - \begin{pmatrix} G^{11} & G^{12} \\ G^{21} & G^{22} \end{pmatrix}\begin{pmatrix} \gamma_1 & 0 \\ 0 & \gamma_2 \end{pmatrix} \times \begin{pmatrix} |\Phi^1\rangle \\ |\Phi^2\rangle \end{pmatrix} = \begin{pmatrix} |\phi^1\rangle \\ |\phi_2\rangle \end{pmatrix}, \tag{43}$$

and the amplitudes of reflection rate and the transmission rate are given by

$$r_b = \mathrm{i}\frac{2\pi M}{P}\begin{pmatrix} \langle\psi^1| & \langle\psi^2| \end{pmatrix}\begin{pmatrix} \gamma_1 & 0 \\ 0 & \gamma_2 \end{pmatrix}\begin{pmatrix} |\Phi^1\rangle \\ |\Phi^2\rangle \end{pmatrix}, \tag{44}$$

$$t_b = 1 - \mathrm{i}\frac{2\pi M}{P}\begin{pmatrix} \langle\phi^1| & \langle\phi^2| \end{pmatrix}\begin{pmatrix} \gamma_1 & 0 \\ 0 & \gamma_2 \end{pmatrix}\begin{pmatrix} |\Phi^1\rangle \\ |\Phi^2\rangle \end{pmatrix}, \tag{45}$$

where

$$\langle y|\Phi^1\rangle = \langle r_2 y, y|\Phi^+_{P,b}\rangle, \tag{46}$$
$$\langle y|\Phi^2\rangle = \langle -r_1 y, y|\Phi^+_{P,b}\rangle, \tag{47}$$
$$\langle y|\phi^1\rangle = \langle r_2 y, y|P, \phi_b\rangle, \tag{48}$$
$$\langle y|\phi^2\rangle = \langle -r_1 y, y|P, \phi_b\rangle, \tag{49}$$
$$\langle y|\psi^1\rangle = \langle r_2 y, y| - P, \phi_b\rangle, \tag{50}$$
$$\langle y|\psi^2\rangle = \langle -r_1 y, y| - P, \phi_b\rangle, \tag{51}$$
$$\langle x|G^{11}|y\rangle = \langle r_2 x, x|G_0^+(E_p)|r_2 y, y\rangle, \tag{52}$$
$$\langle x|G^{12}|y\rangle = \langle r_2 x, x|G_0^+(E_p)| - r_1 y, y\rangle, \tag{53}$$
$$\langle x|G^{21}|y\rangle = \langle -r_1 x, x|G_0^+(E_p)|r_2 y, y\rangle, \tag{54}$$
$$\langle x|G^{22}|y\rangle = \langle -r_1 x, x|G_0^+(E_p)| - r_1 y, y\rangle. \tag{55}$$

5.1. Free Green function

To numerically evaluate the integral equation (43), we need to calculate the free Green function

$$\begin{aligned}&\langle X, x|G_0^+(E_P)|Y, y\rangle \\ &= \langle X, x|\frac{1}{E_P + E_b - H_0 + \mathrm{i}\epsilon}|Y, y\rangle \\ &= G_0^{(I)} + G_0^{(II)},\end{aligned} \tag{56}$$

where

$$G_0^{(I)} = \int_{-\infty}^{\infty} \mathrm{d}Q \frac{\langle X, x|Q, \phi_b\rangle\langle Q, \phi_b|Y, y\rangle}{E_P - E_Q + \mathrm{i}\epsilon}, \tag{57}$$

$$G_0^{(II)} = \int_{-\infty}^{\infty} \mathrm{d}Q \int_{-\infty}^{\infty} \mathrm{d}p \frac{\langle X, x|Q, \phi_{p^+}\rangle\langle Q, \phi_{p^+}|Y, y\rangle}{E_P - E_Q + E_b - E_p + \mathrm{i}\epsilon}. \tag{58}$$

By detailed calculations (see appendix for more details), the free green function is given by

$$G_0^{(I)} = \mathrm{e}^{-q(|x|+|y|)}\frac{-\mathrm{i}Mq\mathrm{e}^{\mathrm{i}P|X-Y|}}{P}, \tag{59}$$

$$G_0^{(II)} = \frac{\kappa M}{2\pi\mathrm{i}}\int_{-\infty}^{\infty}\mathrm{d}p\left[\left(\mathrm{e}^{\mathrm{i}p|x-y|} + \frac{\mathrm{i}q}{p - \mathrm{i}q}\mathrm{e}^{\mathrm{i}p(|x|+|y|)}\right) \times \frac{\mathrm{e}^{\mathrm{i}\frac{|X-Y|}{\kappa}\sqrt{\kappa^2P^2 - q^2 - p^2}}}{\sqrt{\kappa^2P^2 - q^2 - p^2 + \mathrm{i}\epsilon}}\right]. \tag{60}$$

To further simplify the calculation of G_0^{II}, let

$$p_0 = \sqrt{|\kappa^2P^2 - q^2|}, \tag{61}$$
$$\sigma = \mathrm{sgn}\,\kappa^2P^2 - q^2, \tag{62}$$
$$q_0 = \frac{q}{p_0}, \tag{63}$$
$$\alpha = p_0|x - y|, \tag{64}$$
$$\beta = p_0|X - Y|/\kappa, \tag{65}$$
$$\eta = p_0(|x| + |y|), \tag{66}$$
$$z = \frac{p}{p_0}. \tag{67}$$

Then the second term in the free Green function can be rewritten as

$$G_0^{(II)} = \frac{\kappa M}{\pi \mathrm{i}} \int_0^\infty \mathrm{d}z \left(\cos(\alpha z) - \frac{q_0^2 \cos(\eta z) + q_0 z \sin(\eta z)}{z^2 + q_0^2} \right) \times \frac{\mathrm{e}^{\mathrm{i}\beta\sqrt{\sigma - z^2}}}{\sqrt{\sigma - z^2}}. \tag{68}$$

It can be simplified as follows:

Case i: When $\kappa^2 P^2 - q^2 < 0$, $\sigma = -1$, and then

$$G_0^{(II)} = -\frac{\kappa M}{\pi} \int_0^\infty \mathrm{d}u (\cos(\alpha \sinh(u)) - \frac{q_0^2 \cos(\eta \sinh(u)) + q_0 \sinh(u) \sin(\eta \sinh(u))}{\sinh(u)^2 + q_0^2} \Big) \mathrm{e}^{-\beta \cosh(u)}. \tag{69}$$

Case ii: When $\kappa^2 P^2 - q^2 > 0$, $\sigma = 1$, and then

$$\begin{aligned} G_0^{(II)} = & -\mathrm{i}\frac{\kappa M}{\pi} \int_0^{\frac{\pi}{2}} \mathrm{d}u (\cos(\alpha \sin u) \\ & - \frac{q_0^2 \cos(\eta \sin u) + q_0 \sin u \sin(\eta \sin u)}{\sin u^2 + q_0^2} \Big) \cos(\beta \cos u) \\ & + \frac{\kappa M}{\pi} \int_0^{\frac{\pi}{2}} \mathrm{d}u (\cos(\alpha \sin u) \\ & - \frac{q_0^2 \cos(\eta \sin u) + q_0 \sin u \sin(\eta \sin u)}{\sin u^2 + q_0^2} \Big) \sin(\beta \cos u) \\ & - \frac{\kappa M}{\pi} \int_0^\infty \mathrm{d}u (\cos(\alpha \cosh u) \\ & - \frac{q_0^2 \cos(\eta \cosh u) + q_0 \cosh u \sin(\eta \cosh u)}{\cosh u^2 + q_0^2} \Big) \mathrm{e}^{-\beta \sinh u}. \end{aligned} \tag{70}$$

Case iii: When $\kappa^2 P^2 - q^2 = 0$, $\sigma = 0$, and then

$$G_0^{(II)} = -\frac{\kappa M}{\pi} \int_0^\infty \mathrm{d}p (\cos(p|x - y|) - \frac{q^2 \cos(p(|x| + |y|)) + qp \sin(p(|x| + |y|))}{p^2 + q^2} \Big) \frac{\mathrm{e}^{-\frac{p|X-Y|}{\kappa}}}{p}. \tag{71}$$

5.2. Numerical results

Now we are ready to perform the numerical solution of the integral equation (43) to obtain $|\Phi^1\rangle$ and $|\Phi^2\rangle$, and calculate the reflection rate R_b and the transmission rate T_b via equations (44) and (45). The basic method of the numerical calculation involves writing the integral equation (43) in a matrix form by discretizing the position variables and taking a suitable cutoff after checking the numerical convergence, and then solving the eigen problem. The disassociation rate can be obtained by $C_{nb} = 1 - R_b - T_b$ in figure 2, where the parameters are given by $m_1 = m_2 = 1.0$, $\gamma_1 = \gamma_2 = 0.5$, and $\alpha = 2.0$. Compared with the case calculated in the Born approximation, we take larger scattering strengths γ_1 and γ_2 while keeping the other parameters invariant. As expected,

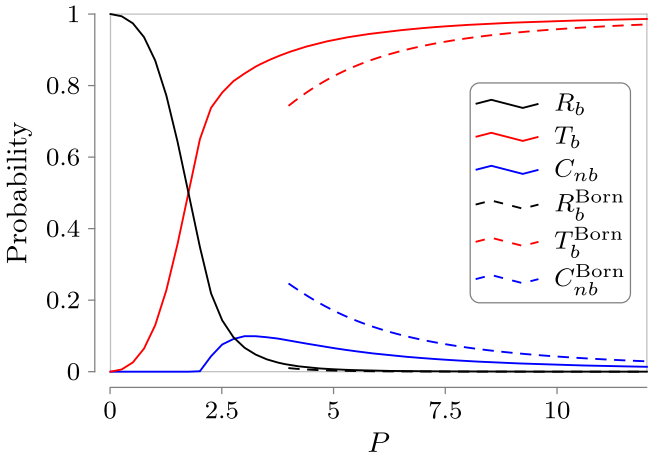

Figure 2. The disassociation rate from numerical solution of the integral equation compared with Born approximation, where the parameters are given by $m_1 = m_2 = 1.0$, $\gamma_1 = \gamma_2 = 0.5$, and $\alpha = 2.0$.

the disassociation channel opens only when the mass-center momentum $P > 2$. With the increase in the momentum P, the transmission rate T_b increases while the reflection rate R_b decreases. The disassociation rate C_{nb} takes its maximum $\simeq 0.1$ at $P \simeq 3.2$. We also show the Born approximation results in the same parameter setting, which become increasingly accurate with the integral results as P increases, just as one can expect.

We also care about how the parameters influence the maximum of the disassociation rate. The disassociation rate depends on the mass of each particle, the interaction strengths $\{\gamma_1, \gamma_2\}$, and the center-of-mass momentum P for a fixed bound strength α. In figure 3, we show that the disassociation rate takes its maximum $C_{nb}^{\max}$ under different parameter settings. The solid black lines in figure 3 show $C_{nb}^{\max}$ with equal interaction strengths $\gamma_1 = \gamma_2 = \gamma$, and equal mass $m_1 = m_2 = 1.0$, while the dashed lines show $C_{nb}^{\max}$ with $m_1 = 0.5$, $m_2 = 1.5$, and different interaction strengths. The bound strength is $\alpha = 2.0$. Figure 3(a) shows the conditions of P and γ when $C_{nb} = C_{nb}^{\max}$, which means that to reach the maximum disassociation rate, one should increase both P and γ by following the relationships revealed in figure 3(a). This relationship between P and γ comes from the constraint that, for a wave packet which has a typical length, larger incoming momentum P takes more energy to disassociate the molecule but also reduces the interaction time with the potential while, during a long interaction time (which means small P), a larger interaction strength γ would cause the oscillation of the reaction procedure. More precisely, from equations (44) and (45) we can calculate the disassociation rate $C_{nb} = A\frac{M\gamma}{P} + B\left(\frac{M\gamma}{P}\right)^2$ (A and B are coefficients containing inner products of scattering states and projective states), which approximates to a quadratic function of $\frac{M\gamma}{P}$ and exists as a maximum. Figure 3(b) gives the values of $C_{nb}^{\max}$ under different parameter settings that change with the interaction strength γ, from which we can see that they increase as γ increases and asymptotically reach some limits. For equal mass and equal interaction strengths, the limit of $C_{nb}^{\max}$ is 0.5. For $\gamma_1 = 5\gamma_2$, the limit is about 0.72, and for $\gamma_2 = 5\gamma_1$, the limit is about 0.75. For

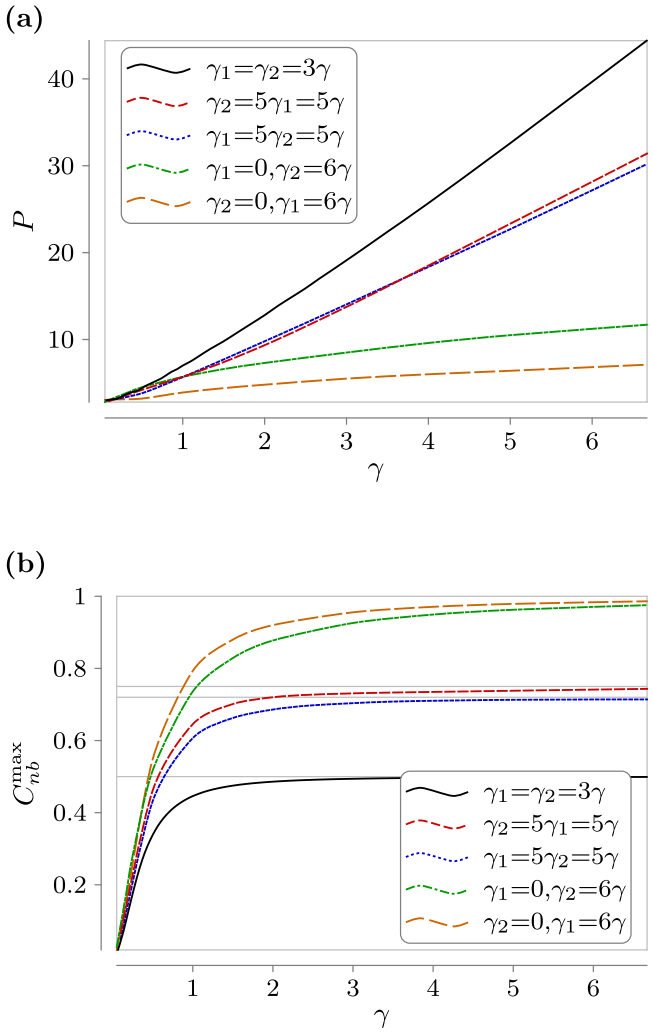

Figure 3. The parameters of the solid black lines are $m_1 = m_2 = 1.0$, $\gamma_1 = \gamma_2 = \gamma$, and $\alpha = 2.0$. The parameters of the dashed lines are $m_1 = 0.5$, $m_2 = 1.5$, and $\alpha = 2.0$. (a) The conditions of center-of-mass momentum P and interaction strengths γ when the disassociation rate C_{nb} takes its maximum $C_{nb}^{\max}$. (b) The maximum of the disassociation rate $C_{nb}^{\max}$ changing with the interaction strengths γ.

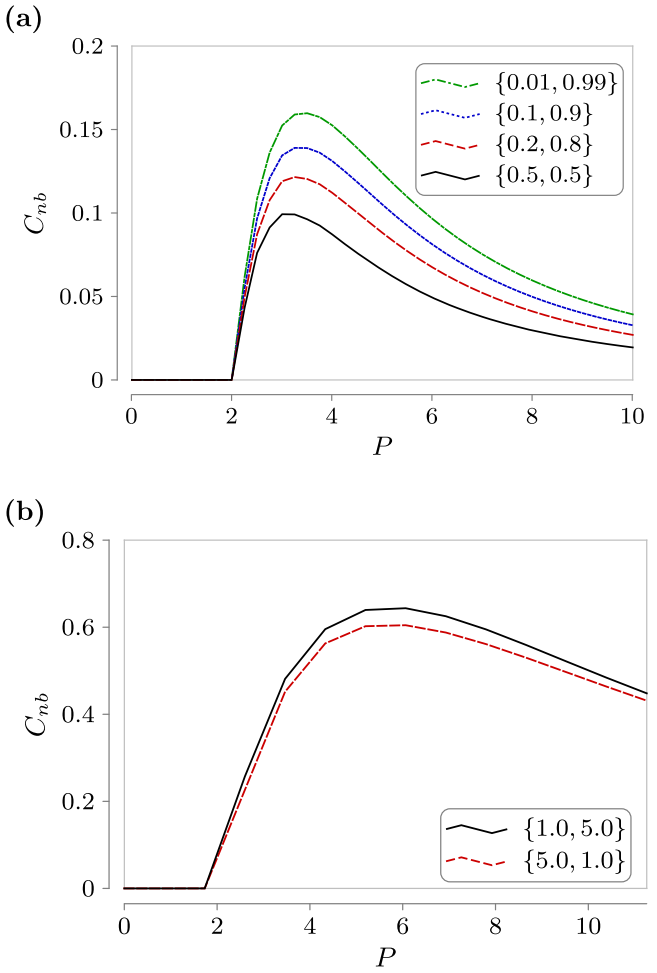

Figure 4. The disassociation rate with different interaction strengths $\{\gamma_1, \gamma_2\}$, where the parameters are given by (a) $m_1 = m_2 = 1.0$, $\alpha = 2.0$ and (b) $m_1 = 0.5$, $m_2 = 1.5$, and $\alpha = 2.0$.

$\gamma_1 = 0$ or $\gamma_2 = 0$, the limit approximates to 1. In conclusion, if one wants to reach a higher disassociation rate, one would tune stronger interaction strengths and center-of-mass momentum by following some similar relations given in figure 3(a) and a larger difference between the interaction strengths γ_1 and γ_2. In fact, this maximum value $C_{nb}^{\max}$ is irrelevant to the coupling strength α in this situation because this can be reduced to a scaling problem.

Meanwhile, for different interaction strengths ($\gamma_1 \neq \gamma_2$), one would suppose that a larger difference between γ_1 and γ_2 would induce a larger disassociation rate. Figure 4 shows more details of the effect, where we keep $\gamma_1 + \gamma_2 = 1.0$ in figure 4(a) to see the main influence of the difference between γ_1 and γ_2. Figures 3(b) 4(b) also show that a lighter particle in the molecule with weaker interaction strength has a higher disassociation rate than that of a lighter particle with stronger interaction strength.

When the coupling of the molecule is strong enough, in the regime of low-injection center-of-mass momentum P the molecule would not disassociate and behave as a single particle. We know the reflection rate R_{single} and transmission rate T_{single} of a single particle scattered by a δ potential, which is a kind of quantum tunneling [24], and in our problem:

$$R_{\text{single}} = \frac{M^2(\gamma_1+\gamma_2)^2}{P^2 + M^2(\gamma_1+\gamma_2)^2}, \tag{72}$$

$$T_{\text{single}} = \frac{P^2}{P^2 + M^2(\gamma_1+\gamma_2)^2}. \tag{73}$$

Figure 5 shows the reflection and transmission rates of the molecule compared with a single particle for $P < 10$, where the parameters are given by $m_1 = m_2 = 1.0$, $\gamma_1 = \gamma_2 = 0.5$, and $\alpha = 12.0$.

6. Discussion and conclusion

In this paper, a simple model with contact interactions, which contains the basic process of disassociation of a one-

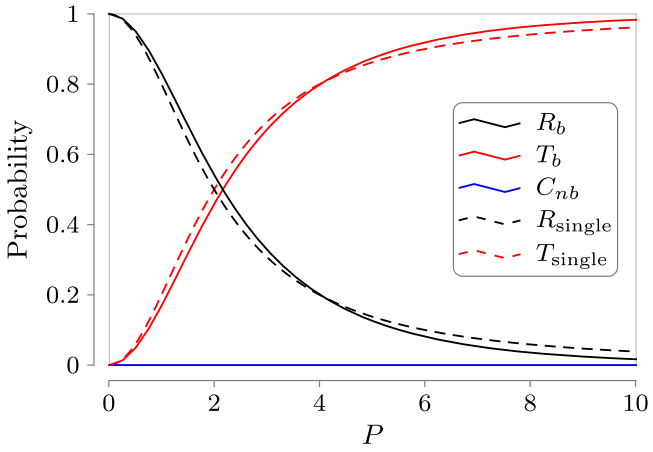

Figure 5. Reflection and transmission rates of the molecule compared with a single particle, where the parameters are given by $m_1 = m_2 = 1.0$, $\gamma_1 = \gamma_2 = 0.5$, and $\alpha = 12.0$.

dimensional molecule, is proposed to describe the corresponding system of ultracold atoms. The first-order Born approximation is made to obtain the basic physical picture of the process: only when the kinetic energy associated with the injection center-of-mass momentum P is larger than the bound energy can the disassociation process occur. To further validate this picture, we develop the numerical method to solve the integral equation of quantum scattering. With the increases in the interaction strengths and the injection center-of-mass momentum, the maximum disassociation rate will increase. With a larger difference between the interaction strengths, the disassociation rate will increase. And under different parameter settings, the maximum disassociation rate has different limits when increasing the interaction strengths and injection momentum.

In the state-of-the-art experiments of ultracold atoms and molecules [15], ultracold bialkali molecules, such as bosonic ^{23}Na^{39}K and ^{23}Na^{87}Rb combined by unequal mass atoms, and Na_2 and K_2 combined by equal mass atoms, can be produced. Optical confinement can be used to constrain the scattering in one dimension. One can move the molecules using optical tweezers or can relatively introduce a moving heavy atom or scattering potential. While putting all the techniques together is not a straightforward endeavor, we see no major roadblock in implementing such a scattering model. We expect that our model can be realized in the experiments of ultracold atoms and molecules in the near future.

Acknowledgments

We thank Peng Zhang for the useful discussions. This work is supported by the National Key Research and Development Program of China (Grant No. 2021YFA0718302 and No. 2021YFA1402104), the National Natural Science Foundation of China (Grant No. 12 075 310), and the Strategic Priority Research Program of the Chinese Academy of Sciences (Grant No. XDB28000000).

Appendix

In this appendix, we show the details of the derivation of equations (59) and (60) giving the free Green function.

The first term of the Green function

$$\begin{aligned}
G_0^{(I)} &= \int_{-\infty}^{\infty} \mathrm{d}Q \frac{\langle X, x|Q, \phi_b\rangle\langle Q, \phi_b|Y, y\rangle}{E_P - E_Q + \mathrm{i}\epsilon} \\
&= \langle x|\phi_b\rangle\langle\phi_b|y\rangle \frac{1}{2\pi}\int_{-\infty}^{\infty} \mathrm{d}Q \frac{\mathrm{e}^{\mathrm{i}Q(X-Y)}}{E_P - \frac{Q^2}{2M} + \mathrm{i}\epsilon} \\
&= \langle x|\phi_b\rangle\langle\phi_b|y\rangle \frac{-2M}{2\pi}\int_{-\infty}^{\infty} \mathrm{d}Q \frac{\mathrm{e}^{\mathrm{i}Q(X-Y)}}{Q^2 - 2ME_P - \mathrm{i}\epsilon} \\
&= \langle x|\phi_b\rangle\langle\phi_b|y\rangle \frac{-2M}{2\pi}\int_{-\infty}^{\infty} \mathrm{d}Q \\
&\times \frac{\mathrm{e}^{\mathrm{i}Q(X-Y)}}{(Q + \sqrt{2ME_P + \mathrm{i}\epsilon})(Q - \sqrt{2ME_P + \mathrm{i}\epsilon})} \\
&= \langle x|\phi_b\rangle\langle\phi_b|y\rangle \frac{-2M}{2\pi} 2\pi\mathrm{i}\frac{\mathrm{e}^{\mathrm{i}\sqrt{2ME_P+\mathrm{i}\epsilon}|X-Y|}}{2\sqrt{2ME_P + \mathrm{i}\epsilon}} \\
&= -\mathrm{i}M\langle x|\phi_b\rangle\langle\phi_b|y\rangle \frac{\mathrm{e}^{\mathrm{i}\sqrt{2ME_P+\mathrm{i}\epsilon}|X-Y|}}{\sqrt{2ME_P + \mathrm{i}\epsilon}} \\
&= \langle x|\phi_b\rangle\langle\phi_b|y\rangle \frac{-\mathrm{i}M\mathrm{e}^{\mathrm{i}P|X-Y|}}{P} \\
&= \mathrm{e}^{-q(|x|+|y|)} \frac{-\mathrm{i}Mq\mathrm{e}^{\mathrm{i}P|X-Y|}}{P}.
\end{aligned} \tag{A1}$$

The second term of the Green function

$$\begin{aligned}
G_0^{(II)} &= \int \mathrm{d}Q \int \mathrm{d}p \frac{\langle X, x|Q, \phi_{p^+}\rangle\langle Q, \phi_{p^+}|Y, y\rangle}{E_P - E_Q + E_b - E_p + \mathrm{i}\epsilon} \\
&= \int \mathrm{d}p\langle x|\phi_{p^+}\rangle\langle\phi_{p^+}|y\rangle \int \mathrm{d}Q \frac{\langle X|Q\rangle\langle Q|Y\rangle}{E_P - E_Q + E_b - E_p + \mathrm{i}\epsilon} \\
&= -\mathrm{i}M\int \mathrm{d}p\langle x|\phi_{p^+}\rangle\langle\phi_{p^+}|y\rangle \frac{\mathrm{e}^{\mathrm{i}\sqrt{2M(E_P+E_b-E_p)+\mathrm{i}\epsilon}|X-Y|}}{\sqrt{2M(E_P + E_b - E_p) + \mathrm{i}\epsilon}}.
\end{aligned} \tag{A2}$$

Let

$$F(p) = -\mathrm{i}M\frac{\mathrm{e}^{\mathrm{i}\sqrt{2M(E_P+E_b-E_p)+\mathrm{i}\epsilon}|X-Y|}}{\sqrt{2M(E_P + E_b - E_p) + \mathrm{i}\epsilon}} \tag{A3}$$

$$= \frac{\kappa M}{\mathrm{i}}\frac{\mathrm{e}^{\mathrm{i}\frac{|X-Y|}{\kappa}\sqrt{\kappa^2P^2-q^2-p^2+\mathrm{i}\epsilon}}}{\sqrt{\kappa^2P^2 - q^2 - p^2 + \mathrm{i}\epsilon}}, \tag{A4}$$

where $\kappa = \sqrt{\frac{\mu}{M}}$.

When $x>0$, $y>0$, the above equation becomes

$$\begin{aligned}
&\int \mathrm{d}p\,\langle x|\phi_{p^+}\rangle\langle\phi_{p^+}|y\rangle F(p)\\
&=\frac{1}{2\pi}\int_0^\infty \mathrm{d}p\frac{p^2}{p^2+q^2}\mathrm{e}^{\mathrm{i}p(x-y)}F(p)\\
&+\frac{1}{2\pi}\int_{-\infty}^0 \mathrm{d}p\left(\mathrm{e}^{\mathrm{i}p(x-y)}+\frac{q^2}{p^2+q^2}\mathrm{e}^{-\mathrm{i}p(x-y)}\right.\\
&\left.+\frac{\mathrm{i}q}{p-\mathrm{i}q}\mathrm{e}^{\mathrm{i}p(x+y)}+\frac{-\mathrm{i}q}{p+\mathrm{i}q}\mathrm{e}^{-\mathrm{i}p(x+y)}\right)F(p)\\
&=\frac{1}{2\pi}\int_0^\infty \mathrm{d}p\left(\frac{p^2}{p^2+q^2}\mathrm{e}^{\mathrm{i}p(x-y)}\right.\\
&\left.+\frac{q^2}{p^2+q^2}\mathrm{e}^{\mathrm{i}p(x-y)}+\frac{\mathrm{i}q}{p-\mathrm{i}q}\mathrm{e}^{\mathrm{i}p(x+y)}\right)F(p)\\
&+\frac{1}{2\pi}\int_{-\infty}^0 \mathrm{d}p\left(\mathrm{e}^{\mathrm{i}p(x-y)}+\frac{\mathrm{i}q}{p-\mathrm{i}q}\mathrm{e}^{\mathrm{i}p(x+y)}\right)F(p)\\
&=\frac{1}{2\pi}\int_{-\infty}^\infty \mathrm{d}p\left(\mathrm{e}^{\mathrm{i}p(x-y)}+\frac{\mathrm{i}q}{p-\mathrm{i}q}\mathrm{e}^{\mathrm{i}p(x+y)}\right)F(p)\\
&=\frac{\kappa M}{2\pi\mathrm{i}}\int_{-\infty}^\infty \mathrm{d}p\left(\mathrm{e}^{\mathrm{i}p|x-y|}+\frac{\mathrm{i}q}{p-\mathrm{i}q}\mathrm{e}^{\mathrm{i}p(x+y)}\right)\\
&\times\frac{\mathrm{e}^{\mathrm{i}\frac{|X-Y|}{\kappa}\sqrt{\kappa^2P^2-q^2-p^2+\mathrm{i}\epsilon}}}{\sqrt{\kappa^2P^2-q^2-p^2+\mathrm{i}\epsilon}}.
\end{aligned}\tag{A5}$$

When $x<0$, $y<0$, we have

$$\begin{aligned}
&\int \mathrm{d}p\,\langle x|\phi_{p^+}\rangle\langle\phi_{p^+}|y\rangle F(p)\\
&=\frac{1}{2\pi}\int_{-\infty}^0 \mathrm{d}p\frac{p^2}{p^2+q^2}\mathrm{e}^{\mathrm{i}p(x-y)}F(p)\\
&+\frac{1}{2\pi}\int_0^\infty \mathrm{d}p\left(\mathrm{e}^{\mathrm{i}p(x-y)}+\frac{q^2}{p^2+q^2}\mathrm{e}^{-\mathrm{i}p(x-y)}\right.\\
&\left.+\frac{\mathrm{i}q}{p-\mathrm{i}q}\mathrm{e}^{-\mathrm{i}p(x+y)}+\frac{-\mathrm{i}q}{p+\mathrm{i}q}\mathrm{e}^{\mathrm{i}p(x+y)}\right)F(p)\\
&=\frac{1}{2\pi}\int_{-\infty}^0 \mathrm{d}p\left(\frac{p^2}{p^2+q^2}\mathrm{e}^{\mathrm{i}p(x-y)}\right.\\
&\left.+\frac{q^2}{p^2+q^2}\mathrm{e}^{\mathrm{i}p(x-y)}+\frac{\mathrm{i}q}{p-\mathrm{i}q}\mathrm{e}^{-\mathrm{i}p(x+y)}\right)F(p)\\
&+\frac{1}{2\pi}\int_0^\infty \mathrm{d}p\left(\mathrm{e}^{\mathrm{i}p(x-y)}+\frac{\mathrm{i}q}{p-\mathrm{i}q}\mathrm{e}^{-\mathrm{i}p(x+y)}\right)F(p)\\
&=\frac{1}{2\pi}\int_{-\infty}^\infty \mathrm{d}p\left(\mathrm{e}^{\mathrm{i}p|x-y|}+\frac{\mathrm{i}q}{p-\mathrm{i}q}\mathrm{e}^{\mathrm{i}p|x+y|}\right)F(p).
\end{aligned}\tag{A6}$$

When $x>0$, $y<0$, we have

$$\begin{aligned}
&\int \mathrm{d}p\,\langle x|\phi_{p^+}\rangle\langle\phi_{p^+}|y\rangle F(p)\\
&=\frac{1}{2\pi}\int_0^\infty \mathrm{d}p\left(\frac{p}{p-\mathrm{i}q}\mathrm{e}^{\mathrm{i}p(x-y)}-\frac{\mathrm{i}pq}{p^2+q^2}\mathrm{e}^{\mathrm{i}p(x+y)}\right)F(p)\\
&+\frac{1}{2\pi}\int_{-\infty}^0 \mathrm{d}p\left(\frac{p}{p-\mathrm{i}q}\mathrm{e}^{\mathrm{i}p(x-y)}-\frac{\mathrm{i}pq}{p^2+q^2}\mathrm{e}^{-\mathrm{i}p(x+y)}\right)F(p)\\
&=\frac{1}{2\pi}\int_{-\infty}^\infty \mathrm{d}p\frac{p}{p-\mathrm{i}q}\mathrm{e}^{\mathrm{i}p(x-y)}F(p).
\end{aligned}\tag{A7}$$

When $x<0$, $y>0$, we have

$$\begin{aligned}
&\int \mathrm{d}p\,\langle x|\phi_{p^+}\rangle\langle\phi_{p^+}|y\rangle F(p)\\
&=\frac{1}{2\pi}\int_0^\infty \mathrm{d}p\left(\frac{p}{p+\mathrm{i}q}\mathrm{e}^{\mathrm{i}p(x-y)}+\frac{\mathrm{i}pq}{p^2+q^2}\mathrm{e}^{-\mathrm{i}p(x+y)}\right)F(p)\\
&+\frac{1}{2\pi}\int_{-\infty}^0 \mathrm{d}p\left(\frac{p}{p+\mathrm{i}q}\mathrm{e}^{\mathrm{i}p(x-y)}+\frac{\mathrm{i}pq}{p^2+q^2}\mathrm{e}^{\mathrm{i}p(x+y)}\right)F(p)\\
&=\frac{1}{2\pi}\int_{-\infty}^\infty \mathrm{d}p\frac{p}{p+\mathrm{i}q}\mathrm{e}^{\mathrm{i}p(x-y)}F(p)\\
&=\frac{1}{2\pi}\int_{-\infty}^\infty \mathrm{d}p\frac{p}{p-\mathrm{i}q}\mathrm{e}^{\mathrm{i}p|x-y|}F(p).
\end{aligned}\tag{A8}$$

Therefore

$$\begin{aligned}
&\int \mathrm{d}p\,\langle x|\phi_{p^+}\rangle\langle\phi_{p^+}|y\rangle F(p)\\
&=\frac{1}{2\pi}\int_{-\infty}^\infty \mathrm{d}p\left(\mathrm{e}^{\mathrm{i}p|x-y|}+\frac{\mathrm{i}q}{p-\mathrm{i}q}\mathrm{e}^{\mathrm{i}p(|x|+|y|)}\right)F(p).
\end{aligned}\tag{A9}$$

The second term of the free Green function

$$\begin{aligned}
G_0^{(II)}&=\frac{\kappa M}{2\pi\mathrm{i}}\int_{-\infty}^\infty \mathrm{d}p\left(\mathrm{e}^{\mathrm{i}p|x-y|}+\frac{\mathrm{i}q}{p-\mathrm{i}q}\mathrm{e}^{\mathrm{i}p(|x|+|y|)}\right)\\
&\times\frac{\mathrm{e}^{\mathrm{i}\frac{|X-Y|}{\kappa}\sqrt{\kappa^2P^2-q^2-p^2}}}{\sqrt{\kappa^2P^2-q^2-p^2+\mathrm{i}\epsilon}}.
\end{aligned}\tag{A10}$$

ORCID iDs

Wen-Liang Li https://orcid.org/0009-0001-4615-1969

References

[1] Schreck F and Druten K van 2021 Laser cooling for quantum gases *Nat. Phys.* **17** 1296–304
[2] Anderegg L, Augenbraun B L, Bao Y, Burchesky S, Cheuk L W, Ketterle W and Doyle J M 2018 Laser cooling of optically trapped molecules *Nat. Phys.* **14** 890–3

[3] Giorgini S, Pitaevskii L P and Stringari S 2008 Theory of ultracold atomic Fermi gases *Rev. Mod. Phys.* **80** 1215–74
[4] Blume D 2012 Few-body physics with ultracold atomic and molecular systems in traps *Rep. Prog. Phys.* **75** 046401
[5] Fitch N J and Tarbutt M R 2021 Chapter three—laser-cooled molecules *Advances In Atomic, Molecular, and Optical Physics* (New York: Academic) vol 70, 157–262
[6] Safronova M S, Budker D, DeMille D, Kimball D F J, Derevianko A and Clark C W 2018 Search for new physics with atoms and molecules *Rev. Mod. Phys.* **90** 025008
[7] Pezzè L, Smerzi A, Oberthaler M K, Schmied R and Treutlein P 2018 Quantum metrology with nonclassical states of atomic ensembles *Rev. Mod. Phys.* **90** 035005
[8] Bloch I, Dalibard J and Nascimbène S 2012 Quantum simulations with ultracold quantum gases *Nat. Phys.* **8** 267–76
[9] Blackmore J A *et al* 2018 Ultracold molecules for quantum simulation: rotational coherences in CaF and RbCs *Quantum Sci. Technol.* **4** 014010
[10] Gross C and Bloch I 2017 Quantum simulations with ultracold atoms in optical lattices *Science* **357** 995–1001
[11] Beterov I I 2020 Quantum computers based on cold atoms *Optoelectron. Instrum. Data Process.* **56** 317–24
[12] Jaksch D, Cirac J I, Zoller P, Rolston S L, Côté R and Lukin M D 2000 Fast quantum gates for neutral atoms *Phys. Rev. Lett.* **85** 2208–11
[13] Bluvstein D *et al* 2022 A quantum processor based on coherent transport of entangled atom arrays *Nature* **604** 451–6
[14] Heazlewood B R and Softley T P 2021 Towards chemistry at absolute zero *Nat. Rev. Chem.* **5** 125–40
[15] Liu Y and Ni K K 2022 Bimolecular chemistry in the ultracold regime *Annu. Rev. Phys. Chem.* **73** 73–96
[16] Olshanii M 1998 Atomic scattering in the presence of an external confinement and a gas of impenetrable bosons *Phys. Rev. Lett.* **81** 938–41
[17] Guan X W and He P 2022 New trends in quantum integrability: recent experiments with ultracold atoms *Rep. Prog. Phys.* **85** 114001
[18] Yang H, Zhang D C, Liu L, Liu Y X, Nan J, Zhao B and Pan J W 2019 Observation of magnetically tunable Feshbach resonances in ultracold ^{23}Na ^{40}K + ^{40}K collisions *Science* **363** 261–4
[19] Wang X Y *et al* 2021 Magnetic Feshbach resonances in collisions of 23Na40K with 40K *New J. Phys.* **23** 115010
[20] Yang H, Wang X Y, Su Z, Cao J, Zhang D C, Rui J, Zhao B, Bai C L and Pan J W 2022 Evidence for the association of triatomic molecules in ultracold 23Na40K + 40K mixtures *Nature* **602** 229–33
[21] Shaffer J P, Rittenhouse S T and Sadeghpour H R 2018 Ultracold Rydberg molecules *Nat. Commun.* **9** 1965
[22] Köhler T, Góral K and Julienne P S 2006 Production of cold molecules via magnetically tunable Feshbach resonances *Rev. Mod. Phys.* **78** 1311–61
[23] Chin C, Grimm R, Julienne P and Tiesinga E 2010 Feshbach resonances in ultracold gases *Rev. Mod. Phys.* **82** 1225–86
[24] Griffiths D J and Schroeter D F 2018 *Introduction to Quantum Mechanics* (Cambridge: Cambridge University Press) III edn